Preprint 22-092

FROTH LAUNDER MODIFICATION IN 300M^3 FLOTATION CELLS AT KENNECOTT COPPERTON CONCENTRATOR

G. Bermudez, Metso Outotec, Englewood, CO
T. Perkins, Rio Tinto, Riverton, UT
R. Sorensen, Rio Tinto, Riverton, UT
C. Smith, Rio Tinto, Riverton, UT
L. Bartsch, Rio Tinto, Riverton, UT
J. Moyo, Rio Tinto, Riverton, UT
R. Dube, Metso Outotec, Englewood, CO
M. Brändström, Metso Outotec, Englewood, CO

ABSTRACT

The Kennecott Copperton concentrator is currently the bottleneck for the Kennecott operation and several projects have been initiated to increase throughput. This increase in grinding circuit throughput has resulted in a coarser grind size which has impacted flotation circuit recovery.

Metso Outotec 300m^3 forced air tank flotation cells are currently utilized in the rougher flotation circuit at the Copperton concentrator. Higher overall recoveries have been observed on the newer Outotec tank cells compared to the original 85m3 self-aspirated flotation cells they replaced. However, coarse particle flotation response on these large, forced air cells did not show encouraging results when compared to smaller previously installed cells. This coarse recovery loss has been attributed to the longer froth transport duration and transport distance on large cells (100m3 and larger). Cell manufacturers addressed the risks of additional coarse particle losses in large cells by installing concentric circumferential launders and crowders (also called center launders). These are designed to reduce froth transport time and distance in the last cells in rougher stages where low residual floatable minerals causes a lack of froth mobility. The center launders also increase froth crowding, which also helps to increase froth transport velocity and increases copper and molybdenum recoveries.

A trial set of the center launder retrofits were installed on the last three tank cells in one of the parallel rougher flotation rows at Copperton. The launder retrofits were installed at the end of October 2020 and monitored until March 2021. This six-month trial showed statistically significant improvements in copper and molybdenum flotation recoveries through the rougher circuit.

INTRODUCTION

Flotation is a common physicochemical method in mineral processing, it is used to separate economic minerals from gangue. The process is undertaken in machines known as flotation cells and, even though flotation was developed and patented over a century ago, there is still continuous improvement and evolution of the technique.

The design of flotation circuits is often based on the use of mechanical cells, they are broadly accepted by the mining industry because of their ease of control, adaptability, and broad range of available sizes on the market (Wills and Finch, 2016). Mechanical flotation cells have trended in recent years towards larger volumes. This is due to declining head grades and the demand from copper producers to treat ever higher volumes of ore to take advantage of the efficiencies and economic benefits of larger scale operations (Lynch, Harbort and Nelson 2010).

Bigger mechanical flotation cells bring several benefits including less equipment to be maintained, smaller footprint per process ton and simplified operation. Larger cell volumes also brought new challenges in terms of froth management, resulting in more difficult conditions for froth to be transported to the launder lip due to larger surface areas and longer transport distances.

In the last four decades the size of the flotation cell has been increased by more than ten times, which has resulted in increased challenges in froth management (Cole et al., 2012; Mesa and Brito-Parada, 2019). Flotation cells' froth transport characteristics can be consistently correlated with flotation performance, as they affect the time that particles reside in the froth phase and, consequently, the probability that they survive the froth phase; (Li et al., 2014).

Flotation cells' considerable increase in effective volume and froth surface area (FSA) is plotted in Figure 1 using Metso Outotec machine references.

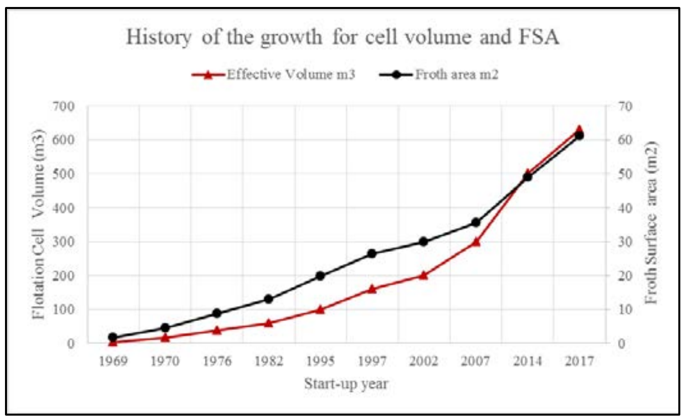

Figure 1. Evolution of flotation tank size and FSA.

Flotation cell volumes larger than 630m^3 have led to a considerable increase of froth mass and a corresponding increase of travel distance to overflow into the launder.

The overall performance of the flotation system is the collective result of pulp zone and froth zone (Rahman et al., 2013). In fact, it wasn't until the late 1980's that Outukumpu (now Metso Outotec) recognized this. The optimization of the flotation performance meant understanding and being able to optimize the performance of each flotation sub-processes (Gronstrand and Kujawa, 2009). A schematic explanation of the two sub-process described by Faltsu and Dobby (1989) is shown in Figure 2 detailing the froth zone recovery (R_cR_f) and its dependence on the collection zone recovery (R_c) and the drop-back (R_c-R_cR_f)); tailings result from losses in the collection zone (1-R_c).

In large flotation cells the role of the froth zone is crucial. In this region the target mineral particles are transported from the cell to form the product concentrate (Rahman, Ata, and Jameson, 2013).

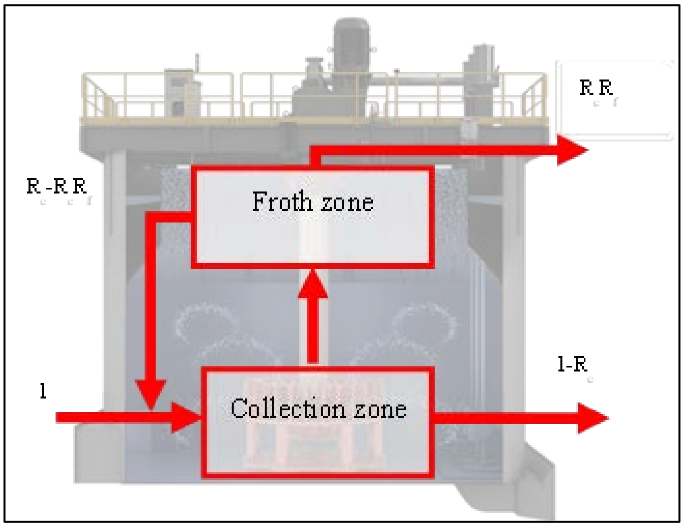

Figure 2. Model for the overall recovery based on collection and froth zone without entrainment.

Froth collection can be affected by modifying the open froth surface area of a cell, having the launder modification can have a direct impact on the metallurgical performance of the retrofitted flotation cell (Grau, et al. 2019). The modified froth zone design incorporates crowders and launders. The launder is a channel where the froth is collected after overflowing a weir. A crowder has the function of improving froth removal by directing the froth towards the launder (Brito-Parada and Cilliers, 2012; Cole et al., 2012). The effect of the launder configuration on froth surface area (FSA) at different tank cells volume was described by Mario Corona (Corona et al, 2021), shown in Figure 3.

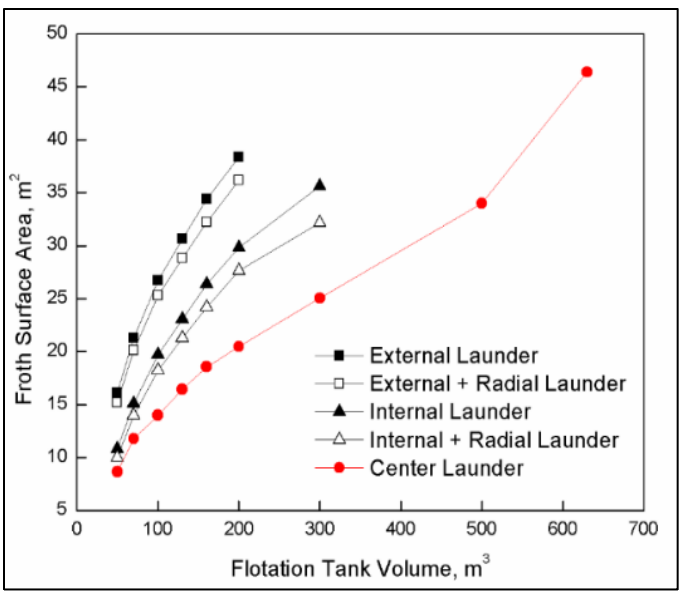

Figure 3. Effect of launder configuration in different tank cells volumes over the froth surface area.

There are not many documented evaluation cases of improved flotation performance in existing cells because of a modification in the open froth area, this is due to three reasons: site flotation circuit's suitable configuration for an evaluation, installation of retrofit flexibility and availability of significant data gathering. One case documented in 2019 in a Cu-Mo concentrator in Peru, retrofitted the last three out of seven TC-300 cells in the rougher circuit with a new center launder configuration, reporting metallurgical recoveries improvements of 0.70% and 1.40% in Cu and Mo respectively (Bermudez. G, et al 2021).

FROTH LAUNDER RETROFIT IN COPPERTON'S 300M^3 FLOTATION TANKCELLS

The Kennecott Copperton concentrator is a 150 ktpd Copper-Molybdenum operation located just outside Salt Lake City, Utah. The operation includes a concentrator, smelter, and refinery. In 2013 the concentrator replaced existing Wemco 85m^3 flotation cells with, new 300m^3 flotation Outotec cells. The new rougher-scavenger circuit consisted of two rows (row 7 & row 8) with five Metso Outotec TankCell300 each. The first two TC-300 work as roughers and the latter three as scavengers. Rougher concentrate feeds the cleaner circuit directly and rougher-scavenger concentrate is also fed to the same circuit post regrinding. Rougher-scavenger tails are final tails.

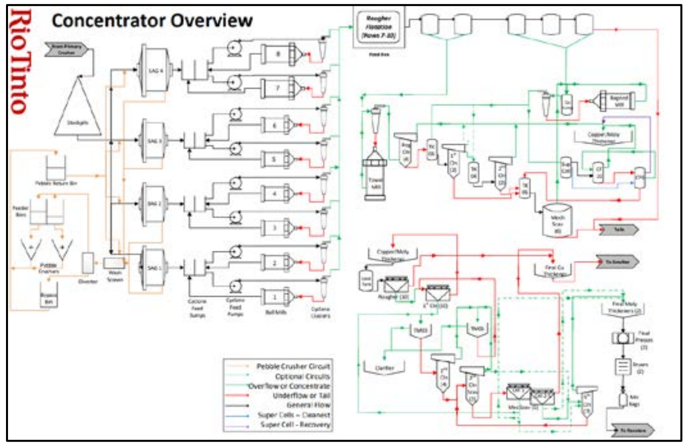

Figure 4. Current Copperton concentrator overview.

After the commissioning of the new flotation circuit, recoveries overall were observed to be higher on the newer Metso Outotec tank cells when compared to the old 85m3 self-aspirated flotation cells. Coarse particle flotation response on the large-forced air cells did not show encouraging results when compared to the smaller cells they replaced. This has been attributed to the longer froth zone characteristics on large cells. Similar behavior was reported during the commissioning of the first Outotec TankCell e500. One of the challenges was that the significant distance of the launder from the tank centerline could lead to poor froth recovery (Murphy, et al., 2015). After Kennecott's site assessment, it was recommended to upgrade froth launders in the scavenger TC-300's with a peripherical internal to center launder.

Figure 5. Rougher-scavenger in Copperton's concentrator, rows 7 and 8.

The main objective of these modifications was to increase froth zone recovery rate to have a positive impact on the flotation circuit's metallurgical efficiency. The center launder upgrade package (Figure 6) has three main components: Froth cone, center launder and outer crowder.

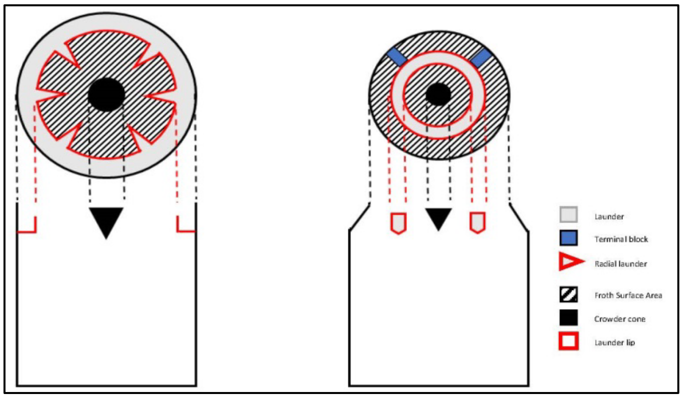

Figure 6. Internal peripherical with 6 radial launder (left) schematic comparison to center launder (right). The left configuration corresponds to original KUC launder design and the right configuration is the upgraded one.

The froth cone aims to ensure froth movement towards the center launder in the inner froth area. The outer crowder pushes the froth contained in the outer froth area towards the center launder so increase froth carry rate and collect all the recovered minerals to the next process stage.

Specific mechanical modification applied to the three retrofitted TankCells-300 are detailed in Table 1 (see APPENDIX), describing Froth Surface Area (FSA), Lip Length (LL), Transport Distance (TD) and crowding:

The new froth surface area consists of two regions, this way significantly decreasing froth transport distance. Crowding in the froth zone resulted in slightly more than double the crowding from 25.8% to 53.6%. Lip length was also decreased from 36.9 m to 23.9 m. The set of three center launder packages were installed at the end of rougher row 8 in October 2020 allowing for the metallurgical evaluation of row 8 relative to its parallel row 7 with non-retrofitted TankCells.

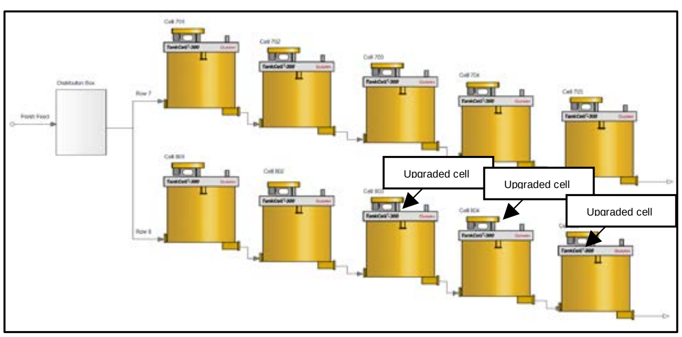

Figure 7. Flotation circuit in KUC subject to metallurgical evaluation.

METALLURGICAL EVALUATION

Individual row recovery calculations are feasible due to independent automatic samplers, head and tailings streams of each row; the effect of the rougher concentrate was not taken into account during this evaluation due to the lack of samplers in those streams. However, because of the inherent noise introduced to the process by multiple variables including reagent dosage, particle size distribution and head grade the direct comparison of both rows' performance would not be adequate. As rows 7 and 8 are parallel we can accept that these changes affect equally the two rows, henceforth, a significant statistical evaluation is possible by comparing recovery of row 8 relative to row 7 before and after the froth launder retrofit.

The 12-hours shift data composite collected from the automatic metallurgical samplers for each stream was collected individually and used in performance calculations. These shift composite samples were then analyzed for Cu and Mo among other elements.

Figure 8. Photo comparison between both launder configurations, radial launders (top) and center launder (bottom).

Approximately 50% of the shift-data points were excluded from the analysis, the three filters were:

- Simultaneous testing with another flotation technology occurring in row 7 during that shift
- Recovery differences between row 8- row 7 >±40%
- Shifts data without assays

Recovery in each valid data point was calculated using the two-product formula applied to Cu and Mo assays (**Equation 1)**:

$$R = \frac{(f-t)}{f} \qquad \text{(Eq. 1)}$$

The differences of recoveries of Row 8 relative to Row 7 were calculated for each valid shift point. The mean of the difference were then used to calculate the net recovery gain per **Equation 2**:

$$\text{Net recovery gain} = (\bar{R}_{After}) - (\bar{R}_{Before}) \qquad \text{(Eq. 2)}$$

Where:

R_{After} = Difference of the means for Cu recovery during the after retrofit the period ($R_{R8After}$ - $R_{R8After}$)

R_{Before} = Difference of the means for Cu recovery during the baseline period ($R_{R8Before}$ - $R_{R7Before}$)

RESULTS AND DISCUSSIONS

Net recovery gain for row 8 relative to row 7 was 0.74% for copper and 0.82% for molybdenum (see APPENDIX - Tables 2 and 3).

Note that before the launder modification there existed a slight tendency for row 8 to underperform row 7, after the launder retrofit this tendency was significantly reduced for Cu and, in the case of Mo, row 8 outperforming row 7. Recoveries were also observed to be more consistent after the upgrade for both Cu and Mo as visualized in Figure 9. It is important to note that around 10% less data sample points were observed during baseline conditions, 114 for the baseline condition and 126 for the upgraded condition.

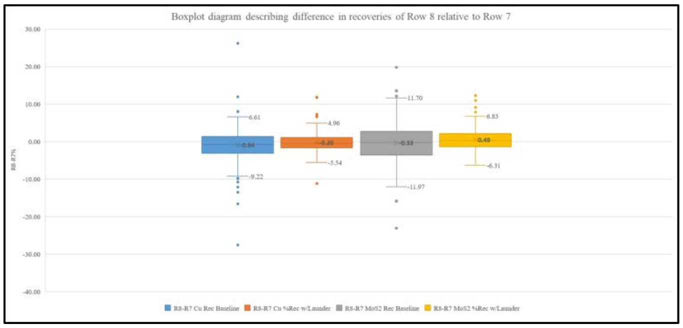

Figure 9. Cu recovery difference of Row 8 relative to Row 7 during the evaluation period.

Head grade has a strong correlation with recovery, and it can be seen in Figure 10 and Figure 11 that row 8 with new center launders has higher recoveries at the same head grade compared to row 7 for both Copper and Molybdenum.

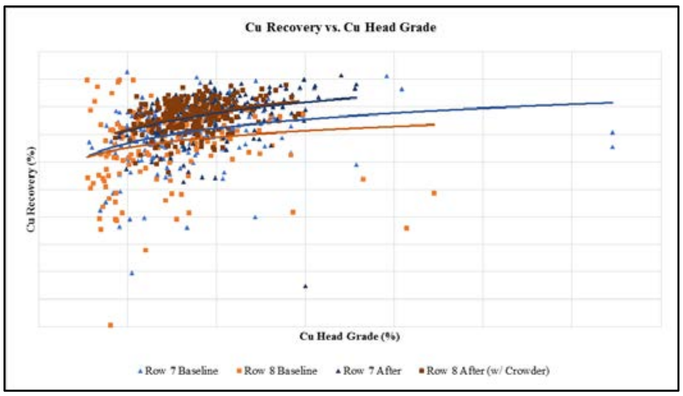

Figure 10. Effect of Cu head grade on Cu recovery for both lines during both evaluation periods.

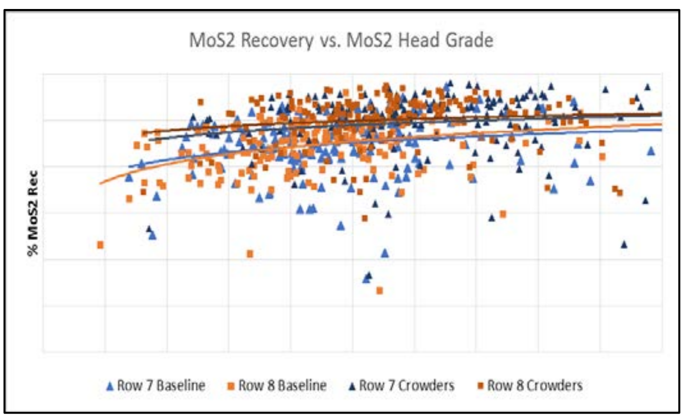

Figure 11. Effect of Mo head grade on Mo recovery for both lines during both evaluation periods.

A statistical evaluation using the two-sample assuming equal variances t-test was undertaken. Note that the sizes of the means can be different for this exercise. Table 4 and Table 5 (see APPENDIX) detail the t-test, resulting in confidence level of 89.8% and 90.8% for Cu and Mo respectively.

As observed in Tables 4 and 5, based in the two-sample t-test assuming equal variances applied to the differences of metallurgical recoveries of Cu and Mo of row 8 relative to row 7, the significance level is average 90%, indicating that this comparison study is statistically significant.

EFFECT IN OPERATING PARAMETERS

After the installation of the new froth launders, new operating conditions were observed for the new froth zone. When comparing the baseline conditions relative to the upgraded conditions within the evaluation period. Note that blank or missing shift data points were removed from the analysis.

Operating airflow rates resulted in smaller volumes after the retrofit looking to maintain similar superficial gas velocity (Jg) in froth in the new smaller froth surfaces areas. Airflow rates were reduced by an average of 26%, 28% and 24% for cells 803, 804 and 805 respectively (Table 6, see APPENDIX). The effect of decreased airflow on the blower's energy consumption is yet to be considered.

On the other hand, looking to restrain gangue recovery, deeper froth beds were set in the three studied cells looking to drain undesirable material back to the collection zone. After the froth launder upgrade, froth bed depth increased by an average of 22%, 35% and 22% for cells 803, 804 and 805 respectively.

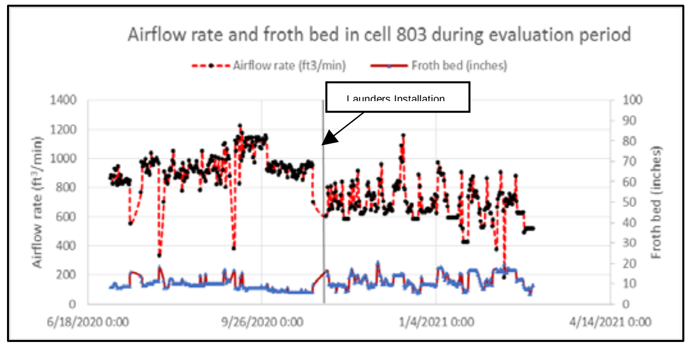

Figure 12. Change in air flow rate and froth bed over time, before and after the center launder installation in cell 803.

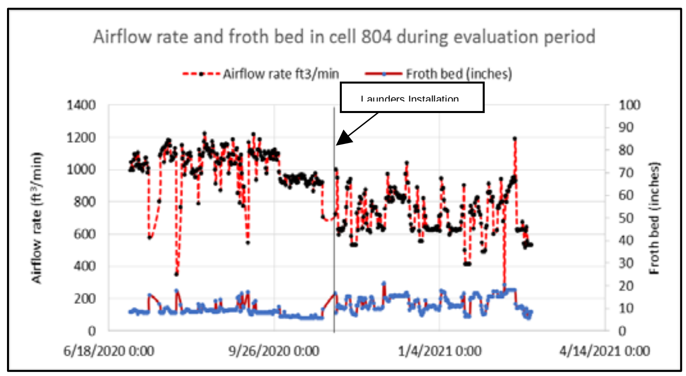

Figure 13. Change in air flow rate and froth bed over time, before and after the center launder installation in cell 804.

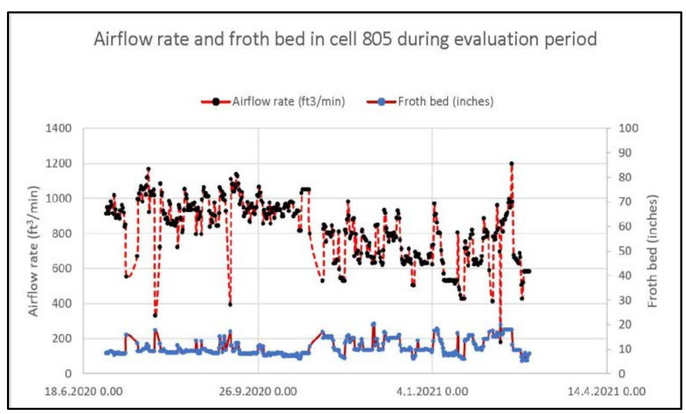

Figure 14. Change in air flow rate and froth bed over time, before and after the center launder installation in cell 805.

CONCLUSIONS

The following conclusions can be drawn from the installation of the center froth launders:

- The concentrate launder upgrade drastically reduced froth transport distance to a third of its maximum value and increased to double the amount of crowding.
- A metallurgical performance improvement was observed during the evaluation period of 0.74% in Cu and 0.81% in Mo for the rougher-scavenger row 8 relative to its mirror parallel row 7.
- Recoveries values for Cu and Mo were observed to be more consistent during the upgraded evaluation period relative to the baseline evaluation period.
- Operating parameters were affected due to the launder retrofit; airflow rate was in general observed to be reduced, impacting positively in blower's energy consumption. Froth beds were deeper after the retrofit, which the authors believe have led to better process control
- The results were statistically significant.

REFERENCES

BERMUDEZ, G., AMELUNXEN, P., MEDINA, M., TAYLOR, M., DUBE, R. (2021). Copper and molybdenum recovery increased by upgrading flotation cells with center launders at Hudbay Constancia. SME Annual Meeting (pp. 1-5). Denver: SME.

BRITO-PARADA, P.R., XU, C., NEETHLING, S.J., and CILLIERS, J.J. (2012). Experimental Studies and Numerical Model Validation of Overflowing 2D Foam to Test Flotation Cell Crowder Designs. Chemical Engineering Research and Design, 2196–2201.

COLE, K. E., BRITO-PARADA, P.R., XU, C., NEETHLING, S.J., and CILLIERS, J.J. (2012). Experimental Studies and Numerical Model Validation of Overflowing 2D Foam to Test Flotation Cell Crowder Designs. Chemical Engineering Research and Design, 2196–2201.

CORONA, M., BERMUDEZ, G., DUBE, R., JALILI, A. (2021). Recent advances in flotation cell froth management. CIM Virtual Convention and Expo. Westmount: CIM Journal.

FALUTSU, M., DOBBY, G. (1989). Direct measurement of froth performance in a laboratory column. In S. R. G.S. DOBBY, Processing of Complex Ores (p. 335). New York: Pergamon Press.

GRAU, R., DAVOISE D., YANEZ, A., LOPEZ, A. (2019). Optimizing the froth area of large mechanical flotation cells. International Mineral Processing Conference Procemin. Santiago.

GRONSTRAND S.,KUJAWA C. (2019). Outotec Flotation Technology – After the Invention of the TankCell®. Mining Magazine Congress. Niagara-on-the-Lake: Mining Magazine.

LI, CHAO FARROKHPAY, SAEED & RUNGE, KYM & BRADSHAW, DEE. (2014). A critical analysis of froth transportation models in flotation. IMPC 2014 - 27th International Mineral Processing Congress (p. Chapter 4). Santiago: impc2014.org.

LYNCH, A.J. WATT, J. S., FINCH, J. A., and HARBORT, G. J. (2017). History of flotation. Melbourne: AusIMM.

MURPHY, B., MATTSSON, T., MAKSIMAINEN, T., MUZINDA, I., RINNE, A. (2016). Performance of the TankCell® e500 at the Kevitsa Mine. SME Annual Conference and Expo: The Future for Mining in a Data-Driven World (p. 563). Phoenix: Society for Mining, Metallurgy, and Exploration.

RAHMAN, R. M., ATA, S., JAMESON, G.J. (2013). Froth Recovery Measurements in an Industrial Flotation Cell. Minerals Engineering, 193–202.

WILLS, B. A., FINCH, J.A., BARRY A. (2016). Wills' Mineral Processing Technology (8 ed.). Oxford, UK: Butterworth-Heinemann.

APPENDIX

Table 1. Froth zone characteristics before and after the center launder upgrade.

Cell type	Internal peripherical launder with six radial launders				Center launder upgrade package						
	FSA (m^2)	Max* TD (m)	LL (m)	Crowding (%)	Inner FSA (m^2)	Outer FSA (m^2)	Total FSA (m^2)	Inner TD (m)	Outer TD (m)	Total LL (m)	Crowding (%)
Kennecott TC-300	37.3	2.9	36.9	25.8	5.7	17.6	23.3	0.7	1.0	23.9	53.6

*Maximum transport distance from center of froth cone to internal launder.

Table 2. Net Cu recovery gain during evaluation period.

	Baseline period		Froth launder modification	
	Row 7 recovery	Row 8 recovery	Row 7 recovery	Row 8 recovery
Means (%)	84.36	83.42	88.59	88.39
Delta recovery (R8-R7), (%)	-0.94		-0.2	
Net recovery gain (After - Before), (%)	0.74			

Table 3. Net Mo recovery gain during evaluation period.

	Baseline period		Froth launder modification	
	Row 7 recovery	Row 8 recovery	Row 7 recovery	Row 8 recovery
Means (%)	84.86	84.53	89.54	90.03
Delta recovery (R8-R7), (%)	-0.33		0.49	
Net recovery gain (After - Before), (%)	0.82			

Table 4. Two-sample assuming equal variances t-test undertaken for Cu.

	R8-R7 Cu Rec w/Froth Modification	***R8-R7 Cu Rec Baseline***
Mean	-0.20	-0.94
Variance	7.76	33.95
Observations	126.00	113
Pooled Variance	20.14	
Hypothesized Mean Difference	0.00	***Net recovery gain***
df	237.00	**0.74**
t Stat	1.27	***Confidence level for 1-tail***
P(T<=t) one-tail	0.10	**89.77 %**
t Critical one-tail	1.65	
P(T<=t) two-tail	0.20	
t Critical two-tail	1.97	

Table 5. Two-sample assuming equal variances t-test undertaken for Mo.

	R8-R7 Cu Rec w/Froth Modification	***R8-R7 Cu Rec Baseline***
Mean	0.49	-0.33
Variance	10.70	35.13
Observations	126.00	114
Pooled Variance	22.30	
Hypothesized Mean Difference	0.00	***Net recovery gain***
df	238.00	0.814343323
t Stat	1.33	***Confidence level for 1-tail***
P(T<=t) one-tail	0.09	90.83%
t Critical one-tail	1.65	
P(T<=t) two-tail	0.18	
t Critical two-tail	1.97	

Table 6. Average operating conditions in each of the three studied cells.

	TankCell 803		TankCell 804		TankCell 805	
	Baseline	Upgraded	Baseline	Upgraded	Baseline	Upgraded
Airflow rate (ft^3/min)	865	639	946	683	868	655
Froth bed (inches)	9.8	12.0	9.4	12.7	9.9	12.0